ISSN 2176-5480

22nd International Congress of Mechanical Engineering (COBEM 2013)
November 3-7, 2013, Ribeirão Preto, SP, Brazil

SIMILARITY LAWS FOR AERODYNAMIC PERFORMANCE EVALUATION OF WIND TURBINES

Willmari Dayana Suarez Hernandez
Mauricio Vicente Donadon
Instituto Tecnológico de Aeronáutica, Praça Marechal Eduardo Gomes, 50, Vila das Acácias - CEP 12.228-900 - São José dos Campos - SP - Brasil.
marwill13@hotmail.com / donadon@ita.com

Oliver José Visconti Montero
Ramiro Gustavo Ramirez Camacho
Universidade Federal de Itajubá, IEM, Av. BPS, 1303, B. Pinheirinho, Itajubá - CEP 37.500-903 - MG - Brasil.
ojvisconti@unifei.edu.br / ramirez@unifei.edu.br

Abstract. *This work presents a study that aims to evaluate the aerodynamic performance of a reduce scale wind turbines. Initially, the wind rotor project is developed based on the application of the blade element theory, where specific dimensions are defined based on the nominal speed and the blade tip speed ratio. To calculate the flow, a periodic domain was generated considering a single blade only. A computational hybrid mesh was generated with prismatic elements in the wall of the blade. To obtain the 3D numerical solution the software CFX® is used. Results as: shaft power, torque and power coefficient for the prototype and scale model were reported. Finally, the prototype and model performance was evaluated. With the presence of small differences that resulted in the determination of a transposition function using the curves adjustment in Matlab®, it is possible to obtain correlations between the prototype and the scale model in different Reynolds situations. This contribution will be of great aid in the design of wind rotors by determining the power coefficient. However, these affinity laws should be experimentally validated.*

Keywords: *Wind Turbine, Power Coefficient, Affinity.*

1. INTRODUCTION

In the last three decades the continuous growth of the world economy has been driven by a relentless increase in the supply of energy using fossil fuels like oil, coal and natural gas. Currently, the worldwide recognition of the limitation on the supply of fossil fuels due to high oil prices and large energy dependence of modern society, has led to a large-scale effort in the search for economical alternative energy sources, and at the same time comply with the conservation of energy resources and natural environment.

Wind energy is not something new, is one of the oldest forms of energy. The wind driving force existed since antiquity, and at all times has been used as such. The knowledge of the behavior of a wind turbine through experimental tests is very expensive, but very importantly; a way to reduce these costs is to predict through numerical simulation the behavior of a good model to scale.

In order to implement the theoretical foundations regarding the operation of wind turbines, the Research Group on Wind Technology of the Technological Institute of Aeronautics (GPTE / ITA) developed a wide range of computer codes; for the sizing of wind rotor and obtaining blade geometry was used the WT - Design code (Dasilva, 2011; Dasilva and Donadon, 2011). Therein, were given as input, the desired power, the wind speed, the airfoil aerodynamic data, the number of blades, the tip speed ratio, among others. Table 1 shows the design data.

Table 1. Wind Rotor Design Data.

Wind Turbine Power (W)	24000
Wind speed (m/s)	10
Air Density (kg/m^3)	1.225
Tip speed ratio	8
Maximum lift coefficient (Airfoil S814)	1.435
Maximum drag coefficient (Airfoil S814)	0.0082
Angle of attack for maximum lift (Airfoil S814)	14
Number of blades	3

Figure 1 shows the distribution of the blade twist angle along the blade radius of 5.36 m. Figure 2 shows the distribution

ISSN 2176-5480

of the chord length depending on the radius of the blade.

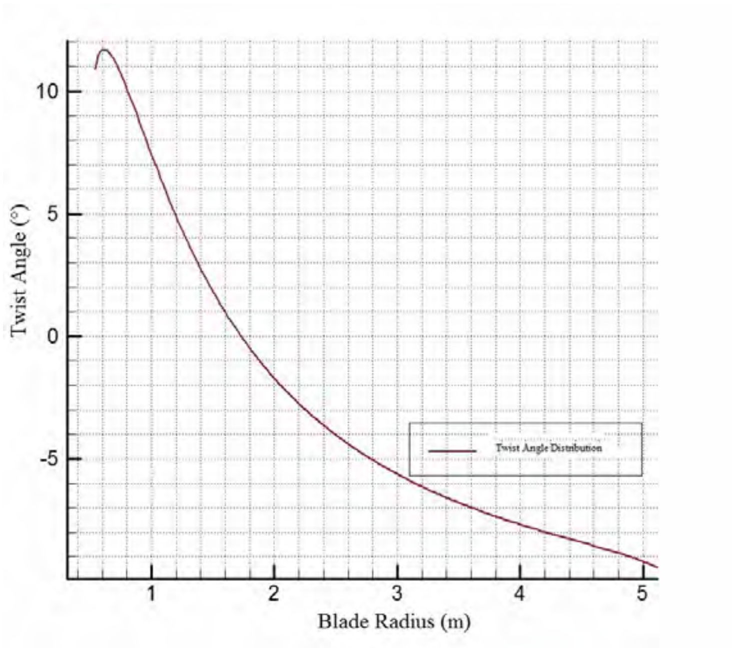

Figure 1. Twist Angle Distribution

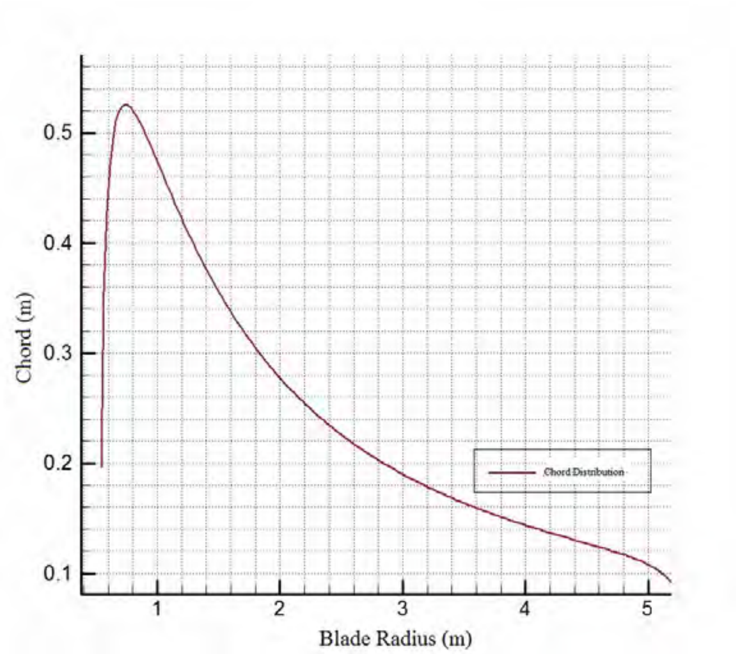

Figure 2. Chord Distribution

Both distributions chord length and twist angle, are regarded as the prototype. According to the laws of geometric similarity, the test model is scaled with respect to the prototype. To ensure the kinematic similarity, it was used the same variation of tip speed ratio (λ) for both prototype and model. To satisfy the dynamic similarity between the prototype and models, in other words, to have the same Reynolds number, the models should be kept spinning at a very high speed, where compressibility effects must be considered and therefore violated the geometric and kinematic similarity. To calculate the flow field it was used the software CFX to obtain behavior characteristic curves of the prototype and models. Finally a method for transposing the power coefficient was determined to adjust the relationship between prototype and models.

ISSN 2176-5480

2. NUMERICAL SIMULATION

The design of the parts of the prototype wind turbine (blade and hub) was performed in CATIA V5R18. Figure 3 shows the blade divided into 20 sections with the same airfoil (S814) in every section, different twist angles and chords according the results obtained in the WT - Design code.

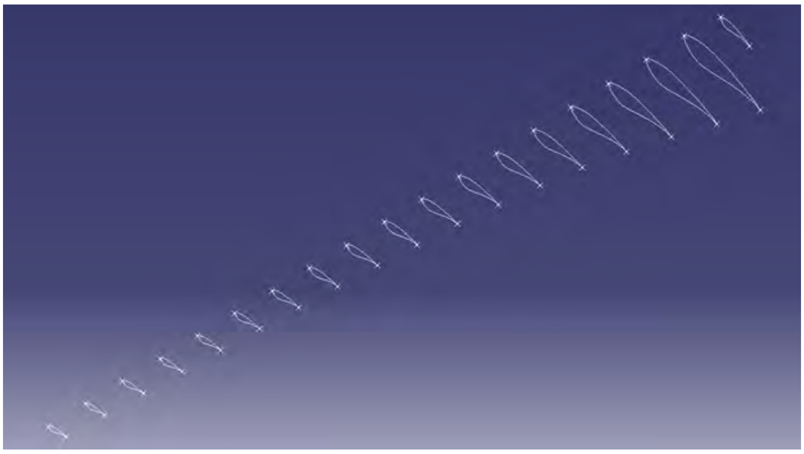

Figure 3. Airfoils along the Blade

Figure 4 shows the control volume that extends in the axial direction 5 radius upstream and 10 radius downstream of the rotor approximately (Carcangiu, 2008). In the plane of the rotor, the domain diameter is two times larger than that of the rotor.

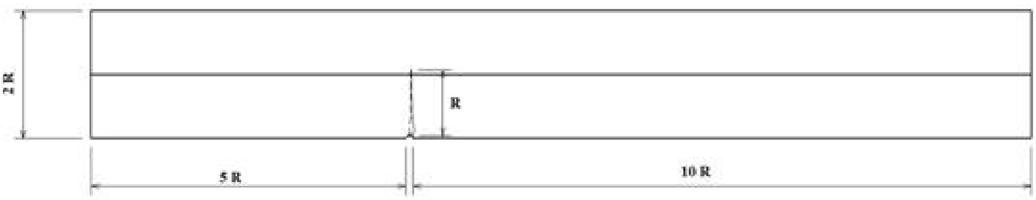

Figure 4. Computational Domain

To generate a volume mesh for the three-bladed rotor, as seen in Fig. 5, a 120 degrees periodicity of the rotor was used, meshing merely the volume around a single blade only. The two remaining blades were included in the calculations using periodic boundary conditions, where the boundary conditions at the inlet and outlet, such as; velocity and static pressure, respectively, were imposed.

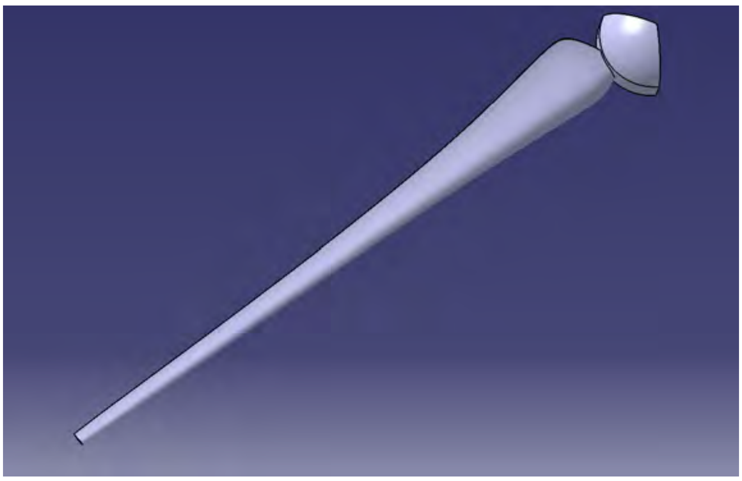

Figure 5. Periodic Blade and Hub in CAD

To calculate the flow, it was generated a hybrid mesh using commercial software ICEM CFD with prismatic elements in the wall of the blade in order to quantify the y + from a region suitable for the calculation of wall tension, on the basis of the Law of the Wall as shown in Fig. 6 and Fig. 7.

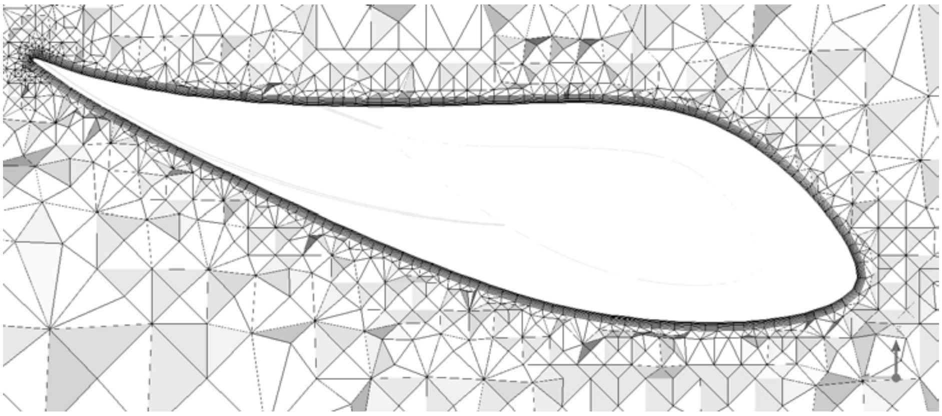

Figure 6. Hybrid Mesh with Prismatic Elements

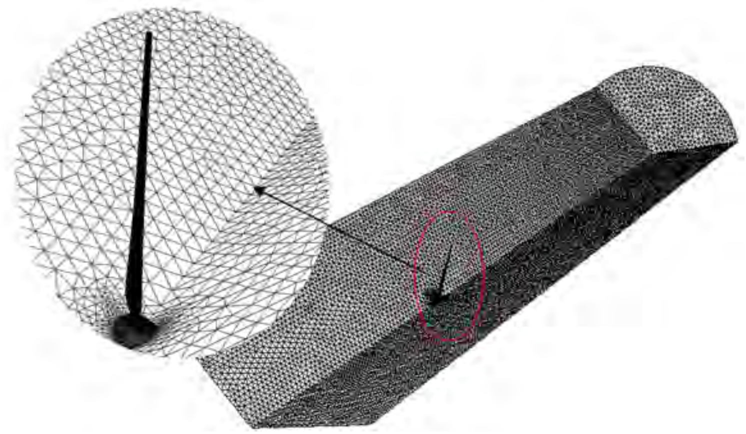

Figure 7. Computational Domain Mesh

2.1 Initial conditions, boundary and turbulence model

As boundary conditions were imposed, the velocity inlet, varying from a range of 5 to 15 m/s, the outlet relative pressure, as zero Pascal and the rotation was set for each scale factor (FE).

The periodic region is defined with an angle of 120 (see Fig. 8), resulting in a single blade in the computational domain.

3. BUCKINGHAM Π THEOREM

Firstly, for the analysis of similarity it was conducted the Buckingham Π Theorem as shown below.

Initially, important parameters are obtained for the problem, N parameters:

Flow properties: V_{∞}
Geometry: D
Fluid Properties: μ, ρ
Other: P_{mec}, ω

where:

$$P_{mec} = \text{f}\ (V_{\infty}, \rho, \text{D}, \mu, \omega)$$

Table 2, specifies each of the parameters involved in a system of the wind turbine.

N is defined as the number of parameters involved, that is to say N = 6; once the number of parameters and the dimensional units are established, continues to the second step.

ISSN 2176-5480

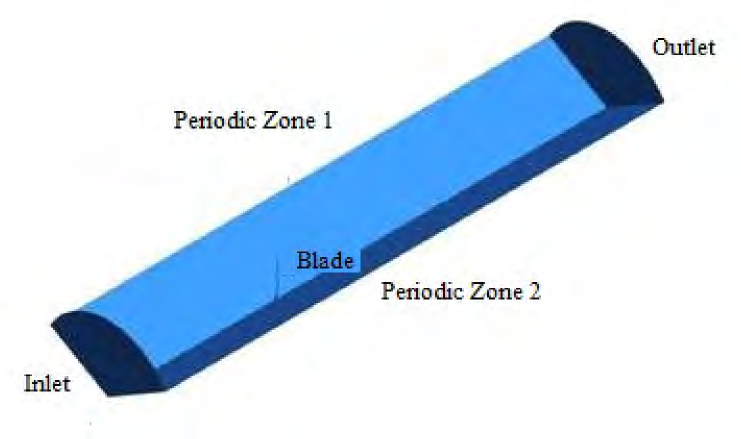

Figure 8. Boundary Conditions

Table 2. Parameters Involved in the System.

P_{mec}	Mechanical Power	W
V_∞	Wind Speed	m/s
ρ	Air density	Kg/m^3
μ	Air Viscosity	Kg/ms
D	Disc Diameter	m
ω	Rotor speed	Rad/s

3.1 Basic Dimensions

In this step, the involved parameters are expressed in terms of primary dimensions. K is defined as the number of primary dimensions present in the problem.

As shown in Tab. 3, the number of primary dimensions is K = 3.

Table 3. Primary Dimension of the System Parameters.

P_{mec}	ML^{2}T^{-2}	W
V_∞	LT^{-1}	m/s
ρ	ML^{-3}	Kg/m^3
μ	ML^{-1}T^{-1}	Kg/ms
D	L	m

3.2 Determination of the number of dimensionless parameters.

The number of dimensionless equations is equal to the number of parameters less the number of primary dimensions present in the problem, namely as in Eq. (1):

$$\Pi = (N - K) = 3 \tag{1}$$

To continue, 3 of the 6 original parameters are chosen arbitrarily as basic and along with the other three considered dependents, will form the dimensionless groups. In this case are taken ρ, V_∞ and D as basic and P_{mec}, μ and ω as dependents.

Now the dimensionless groups are as follows:

$$\Pi 1 = f(V_\infty, \rho, \mathrm{D}, P_{mec}) \tag{2}$$

$$\Pi 2 = f(V_\infty, \rho, \mathrm{D}, \mu) \tag{3}$$

$$\Pi 3 = f(V_\infty, \rho, \mathrm{D}, \omega) \tag{4}$$

ISSN 2176-5480

Now, integer exponents are sought, such that the following products are dimensionless:

$$\Pi 1 = f(V_\infty^a, \rho^b, D^c, P_{mec}^1) \tag{5}$$

$$\Pi 2 = f(V_\infty^a, \rho^b, D^c, \mu^1) \tag{6}$$

$$\Pi 3 = f(V_\infty^a, \rho^b, D^c, \omega^1) \tag{7}$$

The dimensionless condition for $\Pi 1$ leads to the following:

$$(\mathrm{LT}^{-1})^a\ (\mathrm{ML}^{-3})^b\ (\mathrm{L})^c\ (\mathrm{ML}^2\mathrm{T}^{-2})^1 = \mathrm{M}^0\mathrm{L}^0\mathrm{T}^0 \tag{8}$$

$a - 3b + c + 2 = 0 \rightarrow c = -2$
$-a - 3 = 0 \rightarrow a = -3$
$b + 1 = 0 \rightarrow b = -1$

Thus, obtaining the dimensionless number:

$$\pi_1 = \frac{P_{mec}}{V_\infty^3 \rho D^2} \rightarrow C_P \tag{9}$$

Doing the similar calculation for each of the obtained dimensionless numbers:
For $\Pi 2$:

$$\left(LT^{-1}\right)^a \left(ML^{-3}\right)^b (L)^c \left(ML^{-1}T^{-1}\right) = M^0L^0T^0 \tag{10}$$

$$\pi_2 = \frac{\mu}{V_\infty \rho D} \rightarrow R_e \tag{11}$$

For $\Pi 3$:

$$\left(LT^{-1}\right)^a \left(ML^{-3}\right)^b (L)^c \left(T^{-1}\right) = M^0L^0T^0 \tag{12}$$

$$\pi_3 = \frac{\omega D}{V_\infty} \rightarrow \lambda \tag{13}$$

The dimensional analysis is a means of simplifying a physical problem employing dimensional uniformity to reduce the number of variables analyzed.

Obviously the theorem cannot offer all the factors of proportionality required, also does not exist an exact functional form of some parts of the formula, however, simplifies significantly the set of expressions from which the data have to be searched for.

4. MODELING

Once established these numbers, it was possible to model. The basic requirement in this process was to achieve geometric, kinematic and dynamic similarity between the test conditions of the prototype and models.

4.1 Geometric Similarity

The geometric similarity requires that all dimensions of the models should be related to corresponding dimensions in the prototype by a constant scaling factor.

Additionally, in the geometric similarity, all angles are preserved, all directions of flow are preserved, and orientation with respect to the neighborhood should be preserved, that is:

Angle of attack of the model = Angle of attack of the prototype

To meet the conditions of geometric similarity, we established a scale factor of 1:8 between the prototype and model.

The scale was fixed in order to make the experimental tests in the Wind Tunnel $N2/TA - 2$ do IAE, which has the following characteristics: speed of 500 k / h, test an area of 6.3 m2, a height of 2.10 m and a width of 3.00 m.

4.2 Kinematic Similarity

A Similarity kinematics is satisfied when the velocities corresponding points in the models and prototype are in the same direction and their magnitudes differ by a constant scaling factor.

Therefore, the flow must have similar patterns of streamlines.

The flow regimes should be the same.

The similarity kinematic conditions are usually found automatically when the conditions of geometric similarity and dynamic similarity are met.

ISSN 2176-5480

4.3 Dynamic Similarity

Happens if the forces on the model and the prototype differ only by a constant scaling factor at corresponding points.

For the complete dynamic similarity between model and prototype, the scale factor of force must be constant, and that would have the following equalities between the dimensionless parameters of the model and prototype:

$$Re_m = Re_p \text{ , } \lambda_p = \lambda_m \text{ e } Cp_m = Cp_p$$

The simultaneous realization of all the above equations leads to the absurdity that the length scale factor is 1, which means that the model is the prototype itself, which means that it is impossible to test a scale model and to preserved the similarityin in all force fields between model and prototype.

To satisfy the dynamic similarity between the model and prototype, that is, to have the same Reynolds number, the model would have to keep spinning at a very high speed, where compressibility effects should be considered, so the geometric and kinematics would be violated.

However, in tests of models of wind turbines what is done is to consider the dimensionless parameter λ as the most important.

5. Similarity Criterion

In order to comply with the similarities mentioned earlier, the simulations were completed as follows, the rotation that was obtained as optimal design in the design code, being 142.5 rpm was fixed for the prototype. Through the geometric and dynamic similarity, tip speed ratio and diameter ratio; rotation was determined for the model (White, 1998).

It is taken from the dynamic similarity, the blade tip speed ratio equality $\lambda_p = \lambda_m$, where:

$$\lambda_p = \frac{\omega_p R_p}{V} \tag{14}$$

$$\lambda_m = \frac{\omega_m R_m}{V} \tag{15}$$

which it is equal to say:

$$\frac{\omega_p R_p}{V} = \frac{\omega_m R_m}{V} \tag{16}$$

For the same nominal speed variation is:

$$\omega_p R_p = \omega_m R_m \tag{17}$$

Where rotation of the model can be calculated isolating from the Eq. (17):

$$\omega_m = \frac{\omega_p R_p}{R_m} \tag{18}$$

The radius of the model can be calculated as shown in the following equation:

$$R_m = \frac{R_p}{8} \tag{19}$$

Substituting Eq. (19) into Eq. (18), establishes that the rotation of the model is:

$$\omega_m = \frac{\omega_p R_p}{\frac{R_p}{8}} = \omega_m = 8\omega_p = 1140rpm \tag{20}$$

6. Results

To verify the performance of the wind turbine with the hypotheses of this study were carried out numerical simulations.

In order to understand how the wind turbine is behaving, in the simulations were obtained the contours of pressure, relative velocity vectors and streamlines, as shown below:

Figure 9, shows the rotor contours of pressure, obtaining a lower pressure on the blade tip, which is justified by the high speed that is developed at the tip of the blade. Moreover, the well defined contours represent an appropriate mesh configuration and also the residue (10^{-5}) in the solution of the equations of transport.

Figure 10 show the behavior of the relative velocity vectors of the rotor, identifying certainly the direction and the magnitude of velocity.

ISSN 2176-5480

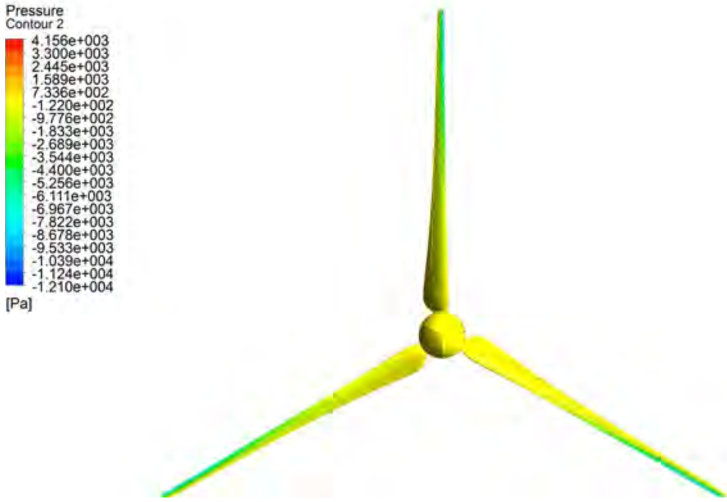

Figure 9. Countours of Pressure

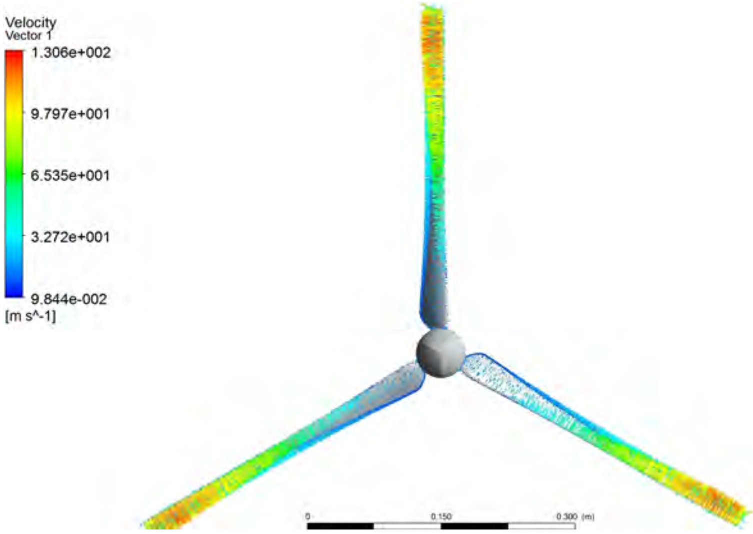

Figure 10. Relative Velocity Vectors

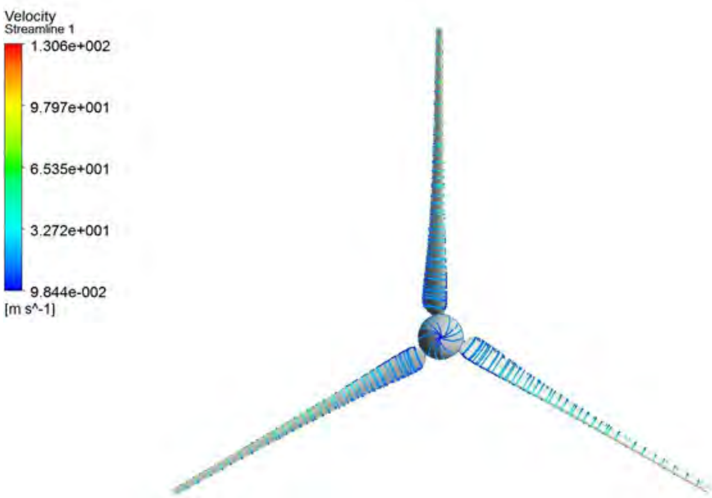

Figure 11. Streamlines on the Surface (Suction Side)

Figure 11 and Fig. 12 show the streamlines projected in the plane of the blade, both the suction side and the pressure side. It appears that the main flow is predominantly along the blade. In the region close to the cube of the pressure side, a secondary flow which does not substantially compromise the efficiency of the rotor in order that the blade tip is the region

ISSN 2176-5480

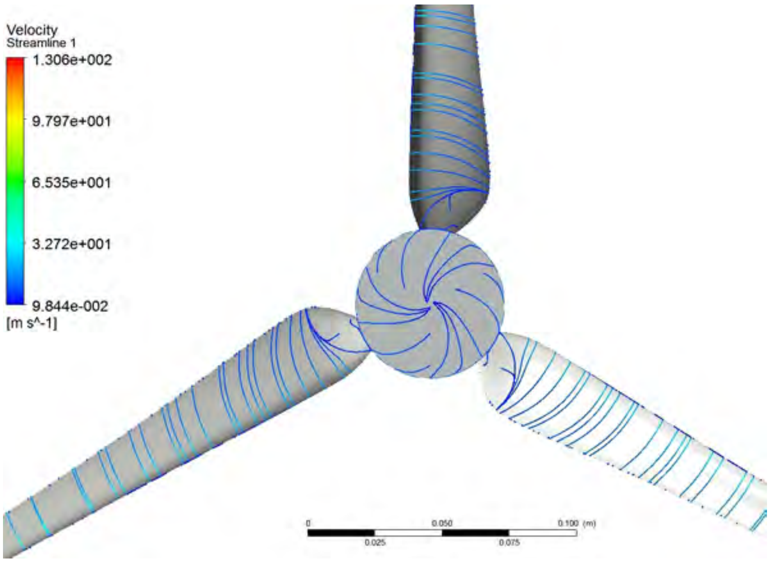

Figure 12. Streamlines on the Surface (Pressure Side)

where the largest portion of kinetic energy is transformed into shaft work.

In Figure 13 it shows the development of streamlines in the downstream flow, showing the formation of forced vortex near the hub.

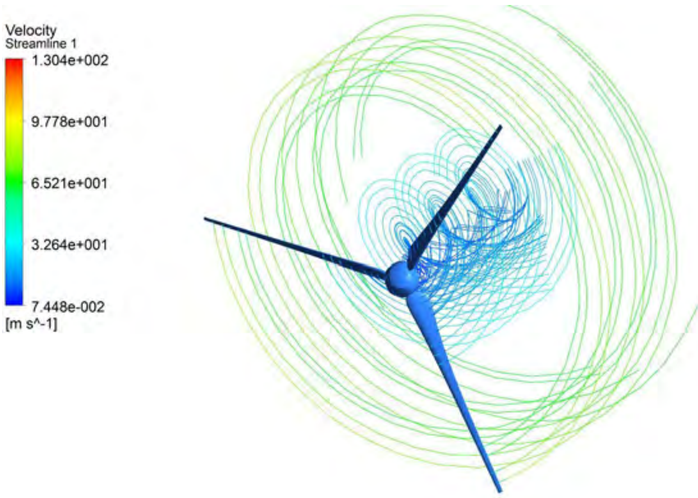

Figure 13. Flow Streamlines

6.1 Transposition Function

The torque was calculated using the torque-z@blade of CFX, and the result used for calculating the power and then to make the calculation of the power coefficient for both cases.

Figure 14 shows the variation of power coefficient as a function of the tip speed ratio (λ).

It can bee seen in the graph shown in Fig. 14 that there is a small difference between the performance of the prototype and the model, that is why a power coefficient methodology of transposition is developed between the data obtained.

The methodology will be established for the variation of the coefficient of power with the rated speed of the turbine.

Both for the model as for the prototype, both changes are similar, showing the same trend, which is also shown in the graph shown in Fig. 15. In the meantime, for situations with higher speeds, the curves tend to coincide, which is justifiable, because the greater the wind speed the greater the reynolds will be; which produces a considerable detachment of the boundary layer on the blades of the generator, acting in a similar way in the prototype and model, causing a decrease between the difference in the performance of both.

To the chart data presented in Fig. 15 it was made a quadratic approximation in the computational language MATLAB, obtaining a variance of 0.9972 for the prototype and 0.9986 for the model. This result was considered acceptable for both cases.

ISSN 2176-5480

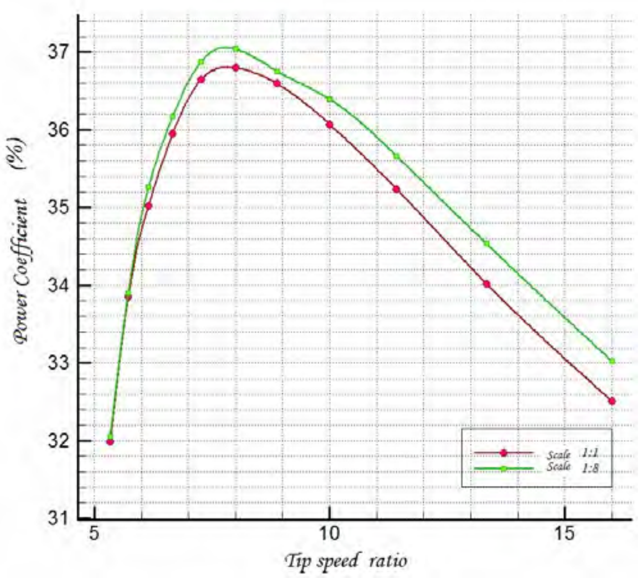

Figure 14. Power coefficient variation.

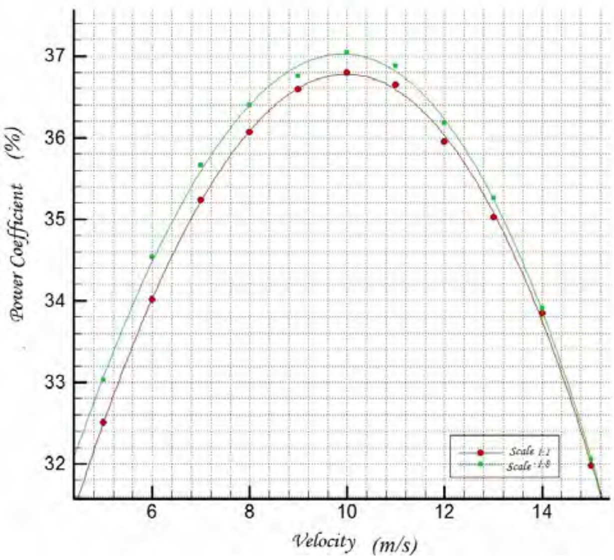

Figure 15. Power coefficient variation with speed.

Table 4 and Tab. 5 show the torque values obtained in CFX and the power shaft calculations of the model and the prototype.

For the prototype it was obtained the following quadratic equation which will be called $f_{prot}(Cp_p, V)$:

$$CP_p = -0,1805V^2 + 3,573V + 19,1 \tag{21}$$

For the model it was obtained the following quadratic equation which will be called $f_{mod}(Cp_m, V)$:

$$CP_m = -0,1779V^2 + 3,477V + 20,04 \tag{22}$$

Once the interpolation functions is obtained, the methodology will be applied to determine the transposition function, which consists in subtracting the approximation function of the model and prototype.

The transpose function is referred to as $f_{trans}(\Delta Cp, V)$, as observed in the graph shown in Fig. 16. The difference between the maximum value of the power coefficient of the prototype and model with the assumptions set, has a value of 0.5 and it is achieved for low wind speeds.

$$f_{trans} = f_{mod} - f_{prot} \tag{23}$$

ISSN 2176-5480

Table 4. Power Curve data of the Prototype

Velocity	λ	Total	Rotation	Shaft	Wind	Power
m/s	-	Torque	(rad/seg)	Power (kW)	Power(kW)	Coefficient
5	15,99	1204,83	14,92	17,97	55,30	32,51
6	13,33	1260,79	14,92	18,81	55,30	34,02
7	11,42	1305,80	14,92	19,48	55,30	35,23
8	9,99	1336,76	14,92	19,94	55,30	36,07
9	8,88	1356,13	14,92	20,23	55,30	36,59
10	7,99	1363,67	14,92	20,34	55,30	36,79
11	7,27	1358,18	14,92	20,26	55,30	36,64
12	6,66	1332,44	14,92	19,88	55,30	35,95
13	6,15	1298,02	14,92	19,36	55,30	35,02
14	5,71	1254,42	14,92	18,71	55,30	33,84
15	5,33	1185,37	14,92	17,68	55,30	31,98

Table 5. Power Curve data of the Model

Velocity	λ	Total	Rotation	Shaft	Wind	Power
m/s	-	Torque	(rad/seg)	Power (kW)	Power(kW)	Coefficient
5	15,99	2,39	119,38	0,28	0,86	33,02
6	13,33	2,49	119,38	0,29	0,86	34,53
7	11,42	2,58	119,38	0,30	0,86	35,65
8	9,99	2,63	119,38	0,31	0,86	36,39
9	8,88	2,66	119,38	0,31	0,86	36,75
10	7,99	2,68	119,38	0,32	0,86	37,03
11	7,27	2,66	119,38	0,31	0,86	36,88
12	6,66	2,61	119,38	0,31	0,86	36,17
13	6,15	2,55	119,38	0,30	0,86	35,26
14	5,71	2,45	119,38	0,29	0,86	33,90
15	5,33	2,32	119,38	0,27	0,86	32,05

$$f_{trans} = C_P = 0,0026V^2 - 0,096V + 0,94 \quad (24)$$

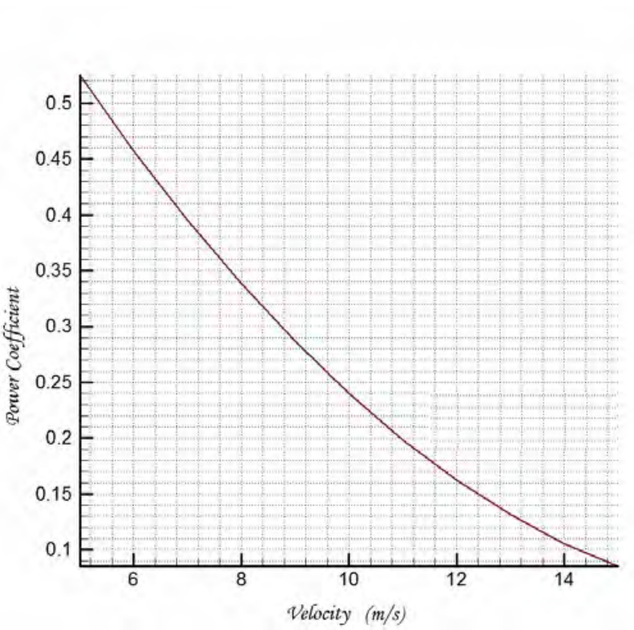

Figure 16. Transposition Function.

7. CONCLUSION

Aiming to develop a similarity criterion for the study of performance of small-scale wind turbines, initially, a dimensional study was developed for the system, understanding as a system, a win turbine subjected to a constant stream of air which we call nominal wind speed.

The dimensionless analysis determined that the most important dimensionless numbers of the system are the power coefficient, the Reynolds number, and the tip speed ratio. After conducting this analysis it was possible to establish the criterion of similarity that were tested computationally. The main similarity criterion adopted, was to establish the tip speed ratio as the most important dimensionless parameter.

Once the criterion was determined, a prototype and small scale rotor were simulated. For the determination of the flow field, commercial software CFX was used; in which boundary conditions and periodicity were introduced. To determine the dissipative effects, it was used the $k\epsilon$ turbulence model, which proved to be efficient in the simulations. An approximation curve was determined for the model and prototype for different nominal speeds of the free stream. Based on these curves, an affinity quadratic equation was obtained between prototype and model; equation that will allow the transposition of data between them when working with the geometry and scales used for this study.

It is important to emphasize that the major contribution of this work is precisely the determination of the criterion to make the simulation and to determine the power coefficient transposition function between the model and prototype. This, will decreases the experimental tests work time, since it will allow the transposition of data between them; decreasing project costs and enabling the development of more efficient wind turbines with the possibility to test changes in the characteristics of the project quickly and efficiently. Meanwhile, these transposing criterions should be validated experimentally.

8. ACKNOWLEDGEMENTS

The authors thank FAPEMIG for his contribution to the development of this work.

9. REFERENCES

Carcangiu, C., 2008. *Cfd-rans study of horizontal axis wind turbines*. Ph.D. thesis, Universita degli Studi di Cagliari, Cagliari, Italy.

Dasilva, C., 2011. *Projeto aerodinâmico ótimo de pá de gerador eólico em regime não estacionário*. Ph.D. thesis, Instituto Tecnológico de Aeronáutica, São José dos Campos, Brazil.

Dasilva, C. and Donadon, M., 2011. "A vortex lattice program for steady state aerodynamic analysis of wind turbine blade loads". In *Proceedings of the 21st International Congress of Mechanical Engineering - COBEM2011*. Natal, Brazil.

White, F.M., 1998. *Fluids Mechanics*. McGraw - Hill, Rhode Island, 5th edition.

10. RESPONSIBILITY NOTICE

The authors are the only responsible for the printed material included in this paper.